



Dual-Domain Convergence Criterion for Iterative Digital Predistortion Coefficient Optimization in E-Band mmWave Systems

Tatiana Krasik

Independent Researcher, Orlando, Florida, USA.

Abstract

This letter presents a dual-domain convergence criterion methodology for iterative digital predistortion (DPD) coefficient optimization in E-band (71-86 GHz) mmWave production automated test environments (ATE). Existing stopping criteria rely on a single measurement domain: received signal level (RSL) stability [10] or coefficient delta norms [1]. Both work at low modulation orders. Neither is sufficient at 256QAM. In practice, RSL convergence consistently precedes mean square error (MSE) stabilization at the demodulator, producing a false convergence window during which premature termination yields a miscalibrated radio. The proposed methodology requires both an RF-domain RSL stability condition and a baseband MSE threshold to be satisfied simultaneously before the loop may exit, augmented by a bounded safety exit counter guaranteeing finite execution time. The criterion is formalized for E-band backhaul systems and illustrated numerically under representative production ATE parameters.

Keywords: Digital Predistortion, DPD, Convergence Criterion, E-Band, mmWave, Automated Test, 256QAM, Measurement Methodology.

INTRODUCTION

At mmWave frequencies, power amplifier nonlinearity limits achievable modulation order. DPD is the standard compensation technique [2]. In production ATE, the calibration loop runs as a sub-routine inside a longer test sequence, and the stopping criterion determines whether the loop exits with a properly calibrated radio or a defective one. This letter addresses the question of which metric actually reflects calibration state.

The two single-metric approaches in common production use, RSL stability [10] and coefficient delta norms [1], both have established literature support, but neither directly observes the baseband EVM that determines whether the unit passes its final verification.

E-band (71-86 GHz) backhaul links are among the most challenging mmWave systems to test in production. The combination of 256QAM modulation, multi-gigahertz instantaneous bandwidth, and tight EVM budgets forces the power amplifier well into its nonlinear region, making DPD a practical requirement for meeting EVM and spectral mask specifications [3, 4], not an optional performance enhancement. Every DPD calibration loop must complete within a bounded time and deliver a unit that passes the

downstream EVM check. The convergence criterion is the only mechanism that makes that determination.

The DPD literature has focused on algorithm development: memory polynomial models [5], Volterra-series architectures [6], and per-beam linearisation for phased arrays [2]. The stopping criterion has received far less attention. Ding et al. [7] showed that coefficient norms are poor proxies for EVM in wideband systems. Cripps [8] observed that AM/PM distortion, dominant at mmWave frequencies, scatters the constellation without proportionally changing received power. This decoupling between RSL and MSE is the physical basis of the false convergence failure mode addressed here.

To the best of the author's knowledge, no published work formalises a joint RF-domain and baseband-domain stopping criterion for iterative DPD. This letter proposes one: a dual-domain criterion that watches both RSL and MSE, exits only when both are satisfied, and bounds the loop with a safety counter. A formal guarantee is derived and validated by Monte Carlo simulation. E-band backhaul is the reference environment; parameters are drawn from production ATE practice.

SYSTEM MODEL

The reference system is an E-band (71-86 GHz) point-to-point

Citation: Tatiana Krasik, "Dual-Domain Convergence Criterion for Iterative Digital Predistortion Coefficient Optimization in E-Band mmWave Systems", Universal Library of Engineering Technology, 2026; 3(2): 53-59. DOI: <https://doi.org/10.70315/uloap.ulete.2026.0302010>.

link running 256QAM. The transmit chain includes a power amplifier (PA) characterised by the Saleh behavioural model [11], which captures the AM/AM and AM/PM nonlinearities of saturating amplifiers and is widely used as a generic model for solid-state mmWave PAs:

$$A(r) = \alpha_a \cdot r / (1 + \beta_a \cdot r^2), \quad \Phi(r) = \alpha_p \cdot r^2 / (1 + \beta_p \cdot r^2)$$

Here $r = |x|$ is the instantaneous input envelope, $A(r)$ is the output amplitude (AM/AM characteristic capturing gain compression), and $\Phi(r)$ is the output phase shift (AM/PM characteristic). The model is memoryless: A and Φ depend only on the instantaneous r and not on the input history; weak-memory extensions are discussed in Section VI. Device parameters α_a , β_a , α_p , β_p are from [11]. The predistorter is a memoryless 5th-order polynomial in the input signal retaining only odd-order terms: $y = c_1 \cdot x + c_3 \cdot x|x|^2 + c_5 \cdot x|x|^4$. The complex coefficients c_1 , c_3 , c_5 are updated each iteration by the indirect learning rule [6].

After each coefficient update, the receiver produces two numbers:

RSL - the received signal level at the RF input of the demodulator (dBm), reflecting the aggregate link power condition.

MSE - the mean square error at the demodulator output, computed over a fixed symbol block, reflecting residual distortion after demodulation of the 256QAM constellation.

Each iteration updates the coefficient vector θ , writes it to the device, then reads RSL_n and MSE_n. The loop runs until both conditions clear or n reaches N_{max} .

ATE Production Measurement Chain

In production ATE, RSL and MSE are read from separate instruments or subsystems. RSL comes from the receiver AGC register or a power detector on the demodulator board, sampled once per iteration after a 50-200 ms settling wait. MSE is computed by the demodulator DSP over a fixed symbol block (10 000-100 000 symbols) and returned via GPIB, USB, or Ethernet. The two measurements come from different layers of the receive chain and use different averaging windows. This separation is a normal feature of ATE architecture, not a deficiency, but it means that RSL and MSE can reach their respective steady states at different loop iterations.

The per-iteration latency T_{iter} includes coefficient write time (10-50 ms), RF settling time (100-500 ms), RSL readback, and MSE block acquisition, totalling 0.3-1.0 s per iteration in typical configurations, consistent with Table I. For $N_{max} = 100$ iterations the calibration sub-routine runs 30-100 s. A false convergence that forwards a unit with a miscalibrated predistorter sends it into the downstream test sequence, output power flatness, spurious emissions, ACPR,

where all results are invalid, requiring a full restart. The time cost is not the DPD sub-routine alone but the entire sequence that ran on a defective device [8].

DUAL-DOMAIN CONVERGENCE METHODOLOGY

Single-Domain Criterion Insufficiency

The simplest stopping rule: exit when RSL stops changing. Formally, terminate when

$$\Delta RSL_n = |RSL_n - RSL_{\{n-1\}}| < \delta_{RSL}$$

At lower modulation orders, RSL is a usable proxy for link quality, but at 256QAM it is not. RSL measures aggregate received power, which tracks primarily the linear predistorter gain c_1 . That coefficient is well-conditioned and converges in a small number of iterations. The higher-order coefficients c_3 and c_5 dominate residual nonlinear distortion but contribute little to total received power, so they are harder to estimate and converge more slowly. RSL therefore settles well before MSE does, and in the interval between those two points a single-domain criterion fires too early.

Dual-Domain Criterion Formulation

Two conditions must both hold before the loop exits:

Condition 1 - RF domain (RSL stability):

$$\Delta RSL_n < \delta_{RSL} \quad \text{AND} \quad RSL_n > RSL_{min}$$

Condition 1 serves two roles: $\Delta RSL_n < \delta_{RSL}$ confirms that the linear coefficient c_1 has stabilised; $RSL_n > RSL_{min}$ is a link validity guard that prevents convergence on a signal too weak for reliable demodulation.

Condition 2 - Baseband domain (MSE threshold):

$$MSE_n < \delta_{MSE}$$

where δ_{MSE} is set such that the predistorter contribution to MSE is no longer the dominant error term. The MSE measured at the demodulator output combines residual predistortion error with receive-chain noise; the DPD calibration loop can drive only the predistortion component toward zero, while the receive-chain noise sets an irreducible floor MSE_{floor} . δ_{MSE} must therefore be set above MSE_{floor} to be reachable. In well-designed links, MSE_{floor} is comparable to EVM^2_{max} (the link is built to meet the spec), so δ_{MSE} is conveniently expressed in units of the target EVM squared:

$$\delta_{MSE} = \alpha \cdot EVM^2_{max}, \quad EVM_{max} = 10^{(EVM_{dB}/20)}, \quad \alpha > 1$$

For 256QAM the typical production EVM requirement is -32 dB [3], giving $EVM_{max} \approx 2.5 \times 10^{-2}$ and $EVM^2_{max} \approx 6.3 \times 10^{-4}$. The factor $\alpha > 1$ represents the ratio between δ_{MSE} and MSE_{floor} and is chosen so that the loop converges reliably without chattering against the noise floor; values in the range $\alpha = 8-20$ are typical when $MSE_{floor} \approx EVM^2_{max}$. The value $\delta_{MSE} = 5 \times 10^{-3}$ used in the simulation below corresponds to $\alpha = 8$ and illustrates the false convergence behaviour clearly; tighter δ_{MSE} values (closer to EVM^2_{max})

are used when the link budget allocates additional headroom to predistortion residual, and a separate downstream EVM verification confirms compliance against the system spec.

Loop continuation condition:

The loop continues while:

$$\Delta RSL_n \geq \delta_{RSL} \text{ OR } RSL_n \leq RSL_{min} \text{ OR } MSE_n \geq \delta_{MSE}$$

Safety Exit Counter and Complete Algorithm

N_{max} caps the loop regardless of convergence state. If Conditions 1 and 2 are not simultaneously satisfied within N_{max} iterations, the unit gets an UNCONVERGED flag and goes to diagnostic review. On a healthy link this never triggers. Repeated safety exits on a given station point to a hardware or setup problem, not a software one.

Algorithm 1: Dual-Domain Convergence Criterion for Iterative DPD

Input: δ_{RSL} , RSL_{min} , δ_{MSE} , N_{max}

Output: θ^* (optimized coefficient vector) or F (failure flag)

```

0: Measure RSL_0 (initial RF reading before loop)
1: n ← 1
2: while n ≤ N_max do
3:    $\theta_n \leftarrow f(\theta_{n-1})$  // coefficient update step
4:   Measure RSL_n (RF domain), MSE_n (baseband domain)
5:    $\Delta RSL_n \leftarrow |RSL_n - RSL_{n-1}|$ 
6:   if ( $\Delta RSL_n < \delta_{RSL}$ ) AND ( $RSL_n > RSL_{min}$ ) // Cond. 1
7:     AND ( $MSE_n < \delta_{MSE}$ ) then // Cond. 2
8:     return  $\theta_n$  // converged
9:   end if
10:   $RSL_{n-1} \leftarrow RSL_n$ ; n ← n + 1
11: end while
12: return F // N_max reached
    
```

Formal Convergence Guarantee

Proposition: Let τ_{RSL} denote the time constant of RSL_n stabilisation (Condition 1) and τ_{MSE} the time constant of MSE_n decay toward δ_{MSE} (Condition 2). Define n_1 as the first iteration at which Condition 1 holds. From Section 3.1, $\tau_{RSL} < \tau_{MSE}$ whenever the PA exhibits any saturating AM/AM behaviour, which is the generic mmWave case. Under this condition, $E[MSE_{\{n_1\}}] > \delta_{MSE}$, i.e., Condition 2 is still unsatisfied at the moment Condition 1 first becomes satisfied. In the noise-free limit the single-domain RSL criterion deterministically exits at n_1 ; finite noise only shifts n_1 by a few iterations. When $\tau_{RSL} < \tau_{MSE}$, false convergence is built into the stopping structure itself, not a result of measurement noise or unlucky realisation. The dual-domain criterion is immune by construction: it cannot exit while $MSE_n \geq \delta_{MSE}$.

NUMERICAL ILLUSTRATION

Table I gives the simulation parameters. PA characteristics follow the original Saleh values from [11]; while the absolute numbers are not specific to any E-band device, the structural $\tau_{RSL} < \tau_{MSE}$ behaviour is preserved across realistic parameter ranges, as shown in Section 4.2. The expected MSE trajectory follows the exponential convergence of the indirect learning LMS update [6] toward the optimal predistorter state. The time constant $\tau = 28$ iterations corresponds to the simulation step size $\mu = 0.06$ and the condition number of the input signal autocorrelation matrix at 256QAM, which determines how quickly the higher-order coefficients c_3 and c_5 converge. The instantaneous MSE is noisy around this mean, as visible in Fig. 1(c).

Table I. Simulation Parameters (Saleh PA Model)

Parameter	Value
Frequency band	71-86 GHz (E-band)
Modulation	256QAM
RSL_0 (initial RSL)	-35 dBm (typical)
MSE_0 (initial MSE)	~0.1
δ_{RSL} (RSL stability threshold)	1 dB
RSL_{min} (minimum RSL)	-20 dBm
δ_{MSE} (MSE threshold)	5×10^{-3}

N_max (safety exit counter)	engineer-set; safety margin (typically 1.5-2×) above the expected convergence iteration; e.g., 100-150 for this configuration
Per-iteration interval T_iter	0.3-1.0 s (system-dependent)
Typical convergence (outer iterations)	~100 (~50 s)

Convergence Trajectory

Fig. 1 shows RSL, Δ RSL, and MSE over 100 iterations. During the initial iterations RSL_n is below RSL_{min} because c₁ has not yet boosted the transmitted power into the operational range; the link validity guard in Condition 1 keeps the loop running. RSL_n rises above RSL_{min} and Δ RSL_n drops below δ _{RSL} at iteration 19; Condition 1 is now satisfied. MSE_n = 0.025 at this point, 5× above δ _{MSE} (Condition 2 not met). A single-domain criterion exits here and passes a miscalibrated radio. The dual-domain criterion continues running until MSE_n crosses δ _{MSE} at iteration 70, at which point both conditions hold and the loop exits cleanly.

The false convergence window spans iterations 19 to 70: 51 iterations during which MSE_n remains above δ _{MSE} while Condition 1 is already satisfied. A single RSL criterion stops here and ships a miscalibrated unit. The width of this window depends on the PA operating point. Section 4.2 quantifies how the gap between RSL settling and MSE settling varies with input back-off; the underlying mechanism is the relative conditioning of the higher-order DPD coefficients c₃ and c₅, which is set by the signal statistics at the PA input.

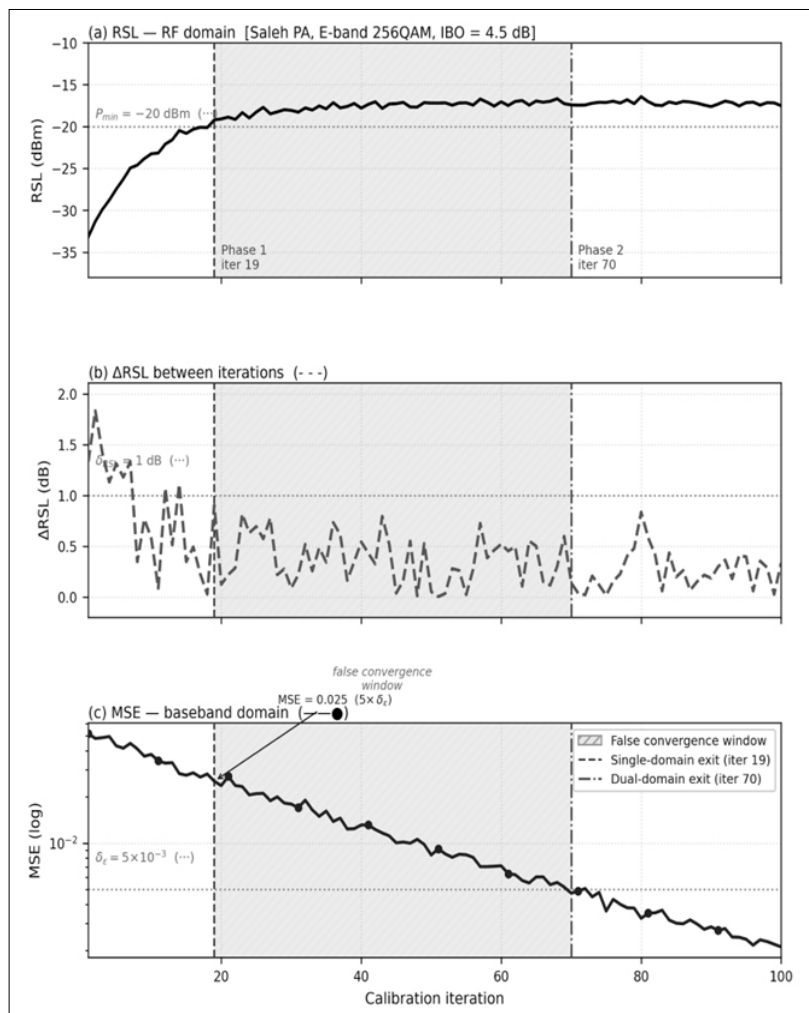


Fig. 1. Simulation results: Saleh PA model ($\alpha_a=2.16$, $\beta_a=0.50$, $\alpha_p=4.00$, $\beta_p=9.10$ [11]), E-band 256QAM. (a) RSL convergence, effective time constant $\tau=9.5$ iter, dominated by c₁ LMS adaptation; AGC settles within a single iteration on this time scale. (b) Δ RSL. (c) MSE exponential decay (LMS, $\tau=28$ iter, $MSE_0=0.052$, $MSE_{opt}=7 \times 10^{-4}$). Single-domain exit: iter 19, $MSE=0.025$ ($5 \times$ above δ _{MSE}). Dual-domain exit: iter 70.

For 256QAM, residual nonlinearity invisible to RSL produces constellation scatter sufficient to degrade EVM. The problem worsens at higher modulation orders: as backhaul moves toward 1024QAM, the gap between RSL and MSE convergence widens.

Parameter Sensitivity Analysis

The simulation was repeated across a range of input back-off (IBO) values, with all other parameters held at their Table I values. IBO sets how deeply the PA is driven into compression: lower IBO means stronger nonlinearity and slower convergence of c_3 and c_5 . Table II shows the false convergence window width and the MSE at the RSL exit point for each IBO.

Table II. False Convergence Window Width vs. Input Back-Off (IBO) at E-Band 256QAM

IBO (dB)	RSL exit (iter)	MSE exit (iter)	Window (iter)	MSE at RSL exit
3.0	14	55	41	0.038 ($7.6 \times \delta_{\text{MSE}}$)
4.5*	19	70	51	0.025 ($5.0 \times \delta_{\text{MSE}}$)
6.0	24	90	66	0.018 ($3.6 \times \delta_{\text{MSE}}$)
8.0	31	120	89	0.012 ($2.4 \times \delta_{\text{MSE}}$)
* Nominal value (Table I). $\delta_{\text{MSE}} = 5 \times 10^{-3}$.				

The window widens as IBO increases (less compression): with weaker nonlinearity the higher-order DPD coefficients c_3 and c_5 are smaller in magnitude, so the LMS gradient signal driving their convergence is correspondingly weaker and τ_{MSE} grows. Crucially, the window never closes: $\tau_{\text{RSL}} < \tau_{\text{MSE}}$ is a structural property of the Saleh model at any operating point that exhibits AM/AM nonlinearity, not an artefact of the nominal simulation conditions. Two limiting cases bracket the behaviour. At IBO = 3 dB the false-convergence window is narrowest (41 iter) but the MSE at the single-domain exit is highest ($7.6 \times \delta_{\text{MSE}}$); the unit ships with the worst miscalibration. At IBO = 8 dB the window is widest (89 iter) but the MSE at the exit is lowest ($2.4 \times \delta_{\text{MSE}}$). The dual-domain criterion captures both cases by construction.

Safety Exit Behaviour and Production Cost of False Convergence

Production test sequences for mmWave backhaul run 30 to 90 minutes per unit, and DPD calibration is a small fraction of that. Its position in the sequence is what matters: if DPD exits early on RSL alone, every stage after it runs on a miscalibrated radio, and the unit either fails final verification or, worse, ships. The cost is not the DPD sub-routine itself but the full test chain that ran after it.

Monte Carlo Validation

We ran 500 Monte Carlo trials, each with a different noise realisation from the same model. Each trial applied both criteria to the same simulated trajectory. Table III summarises the results.

Table III. Monte Carlo False Convergence Rate (N = 500 trials)

Criterion	False conv. rate	Mean MSE at exit	Mean exit iteration
Single-domain (RSL only)	100%	0.028 ($5.6 \times \delta_{\text{MSE}}$)	iter 18
Dual-domain (proposed)	0%	$< \delta_{\text{MSE}}$ (by construction)	iter 69

Row 1: single-domain criterion exits before MSE threshold is met. Row 2: dual-domain criterion exits only after both conditions are satisfied.

The 100% false convergence rate of the single-domain criterion is not a noise artefact. It is a direct consequence of the structural condition $\tau_{\text{RSL}} < \tau_{\text{MSE}}$ established in Section 3. Across all 500 trials, the RSL criterion consistently exited at iteration 18 (± 0.9) with MSE between $4.6 \times$ and $6.6 \times$ above δ_{MSE} . The dual-domain criterion exited at iteration 69 (± 1.5) in every trial, with MSE verified below δ_{MSE} at exit.

Table IV. Comparison of DPD Stopping Criteria for E-Band 256QAM Production ATE

Criterion	Metric	False conv. rate	EVM guarantee	Bounded runtime
RSL stability [10]	RSL only	100%	No	Impl.-dependent
Coeff. delta norm [1]	$\ \Delta\theta\ $	Partial	Indirect	Yes
Direct learning MSE [7]	MSE only	Low	Yes	No
Dual-domain (proposed)	RSL + MSE	0%	Yes (with appropriate δ_{MSE})	Yes (N_{max})

Table IV compares the proposed criterion with published alternatives. The RSL-only criterion [10] provides no EVM guarantee. Coefficient delta norms [1] track an intermediate quantity, not the final quality metric. Direct learning with MSE-only termination [7] guarantees EVM satisfaction but has no upper bound on iteration count, making it unsuitable for production ATE where test time is contractually bounded. The dual-domain criterion is the only approach that satisfies all three conditions simultaneously.

DISCUSSION

The same false convergence window appears in any loop where the RF observable settles faster than the baseband metric, which is the common case at high modulation orders. Ka-band LEO module production and 5G mmWave ATE at 28 and 39 GHz are two examples. Set δ_{MSE} from the target EVM budget; the algorithm transfers without modification. As modulation orders climb toward 1024QAM, the window widens and the dual-domain criterion becomes more necessary, not less.

In Ka-band LEO module production (26.5-40 GHz), the same failure mode occurs with tighter EVM budgets. GaN MMIC devices at 30 GHz exhibit pronounced AM/PM distortion, and Ka-band ATE setups commonly split RSL and EVM measurement across a spectrum analyser and a vector signal analyser, introducing inter-instrument polling latency on top of the structural $\tau_{\text{RSL}} < \tau_{\text{MSE}}$ gap. The dual-domain criterion applies without modification: δ_{MSE} is set from the Ka-band EVM requirement using the same formula in Section 3.2. An analogous structural issue in satellite predistortion is described in [14].

For 5G mmWave base station ATE at 28 GHz (n257, n258, n261) and 39 GHz (n260), beamforming adds complexity. 3GPP TS 38.141-2 specifies EVM per subcarrier group, and a separate DPD loop may run for each beam. RSL aggregates power across multiple spatial streams and is not a per-beam quality indicator; only the per-beam demodulated EVM reflects predistortion state. The dual-domain framework applies directly: RSL_min becomes a per-beam power floor derived from the link budget [12], and δ_{MSE} follows from the 3GPP EVM mask [13]. The N_max counter is particularly important in this context because beamforming instability can produce oscillating RSL that would stall a single-domain criterion indefinitely.

Setting δ_{MSE} , δ_{RSL} , and N_max is straightforward in practice. δ_{MSE} is set using the formula in Section 3.2, with α chosen so that δ_{MSE} comfortably exceeds the receive-chain noise floor MSE_floor; $\alpha = 8$ is a conservative starting point when $\text{MSE_floor} \approx \text{EVM}^2_{\text{max}}$. δ_{RSL} is set above the peak-to-peak fluctuation of the RSL measurement noise (typically 0.5-2 dB in production ATE, i.e., roughly 6σ of the underlying Gaussian); choosing it lower causes $|\Delta\text{RSL}_n|$ to exceed δ_{RSL} on noise alone, which prevents Condition 1 from ever latching. N_max is estimated from the LMS step size μ and the signal condition number, with a $1.5\times$ safety margin. All three values depend on the platform, not on the frequency band; the dual-domain logic is unchanged across systems.

During the author's work on automated test software for E-band backhaul radio modules, repeated instances were observed of units passing the DPD calibration sub-routine, based on RSL stability alone, but failing the subsequent EVM verification step. Root-cause analysis consistently pointed

to the same mechanism described in Section 3.1: the linear coefficient c_1 had settled, RSL appeared stable, and the loop exited, while c_3 and c_5 remained far from their optimal values. The dual-domain criterion was developed from these observations. Implemented as a firmware update to the ATE control software, it eliminated the false convergence failures across all affected unit types without changes to the predistortion algorithm or the hardware test setup, which validates the approach in a commercial production context.

CONCLUSION

Single-domain stopping criteria miss the miscalibration that lives in the baseband: RSL stabilises before MSE does, so stopping on RSL alone leaves the predistortion coefficients in a state that satisfies the RF power check while the demodulator is still miscalibrated. This is the failure mode this work targets.

The fix requires no changes to the predistortion algorithm. A second stopping condition is added in the baseband domain; both conditions must clear before the loop exits, and a counter bounds its runtime. $\tau_{\text{RSL}} < \tau_{\text{MSE}}$ holds for any saturating PA whose higher-order distortion products contribute substantially to constellation error but only marginally to total transmitted power. This separation between RF and baseband convergence rates is structural for memoryless and weakly-memory AM/AM behaviour. For strongly-memory PAs requiring full memory-polynomial DPD, the same mechanism applies, although the analysis must be extended to the augmented coefficient set.

REFERENCES

1. M. Hoflehner and A. Springer, "Early stopping criterion for recursive least squares training of behavioural models," *Wireless Personal Commun.*, 2022, doi: 10.1007/s11277-022-09813-9.
2. A. Brihuela, M. Abdelaziz, L. Anttila, M. Turunen, M. Allén, T. Eriksson, and M. Valkama, "Piecewise digital predistortion for mmWave active antenna arrays: Algorithms and measurements," *IEEE Trans. Microw. Theory Techn.*, vol. 68, no. 9, pp. 4000-4017, 2020.
3. ETSI, "Fixed radio systems; Characteristics and requirements for point-to-point equipment and antennas; Part 2: Digital systems operating in frequency bands from 1 GHz to 86 GHz," Standard EN 302 217-2, European Telecommunications Standards Institute, 2017.
4. FCC, "Millimeter wave propagation: Spectrum management implications," Office of Engineering and Technology, Bulletin No. 70, 2003.
5. D. R. Morgan, Z. Ma, J. Kim, M. G. Zierdt, and J. Pastalan, "A generalized memory polynomial model for digital predistortion of RF power amplifiers," *IEEE Trans. Signal Process.*, vol. 54, no. 10, pp. 3852-3860, 2006.

6. C. Eun and E. J. Powers, "A new Volterra predistorter based on the indirect learning architecture," *IEEE Trans. Signal Process.*, vol. 45, no. 1, pp. 223-227, 1997.
7. L. Ding, G. T. Zhou, D. R. Morgan, Z. Ma, J. S. Kenney, J. Kim, and C. R. Giardina, "A robust digital baseband predistorter constructed using memory polynomials," *IEEE Trans. Commun.*, vol. 52, no. 1, pp. 159-165, 2004.
8. S. C. Cripps, *RF Power Amplifiers for Wireless Communications*, 2nd ed. Norwood, MA: Artech House, 2006.
9. P. B. Kenington, *High-Linearity RF Amplifier Design*. Norwood, MA: Artech House, 2002.
10. R. N. Braithwaite, "Convergence estimation for iterative predistortion factor determination for power amplifiers," U.S. Patent 8,971,829, Mar. 3, 2015.
11. A. A. M. Saleh, "Frequency-independent and frequency-dependent nonlinear models of TWT amplifiers," *IEEE Trans. Commun.*, vol. 29, no. 11, pp. 1715-1720, 1981.
12. ITU-R, "Propagation data and prediction methods required for the design of terrestrial line-of-sight systems," Recommendation P.530-18, International Telecommunication Union, 2021.
13. 3GPP, "NR; Base Station (BS) conformance testing Part 2: Radiated conformance testing," TS 38.141-2 Release 17, 3rd Generation Partnership Project, 2023.
14. R. Piazza, M. R. Bhavani Shankar, and B. Ottersten, "Data predistortion for multicarrier satellite channels based on direct learning," *IEEE Trans. Signal Process.*, vol. 62, no. 22, pp. 5868-5880, 2014.
15. J. Vuolevi and T. Rahkonen, *Distortion in RF Power Amplifiers*. Norwood, MA: Artech House, 2003.